Romanian Reports in Physics, Vol. 66, No. 4, P. 939–951, 2014

NUCLEAR PHYSICS

HEAVY-ION FUSION REACTIONS OF ^{16}O ON SPHERICAL/DEFORMED $^{144\text{-}154}$Sm TARGETS USING COULOMB AND PROXIMITY POTENTIALS

K. P. SANTHOSH[1], V. BOBBY JOSE

Kannur University, School of Pure and Applied Physics, Swami Anandatheertha Campus, Payyanur 670327, India
E-mail[1]: drkpsanthosh@gmail.com

Received January 5, 2014

Abstract. The fusion excitation functions for the fusion of ^{16}O on $^{144\text{-}154}$Sm have been calculated using one dimensional barrier penetration model, taking scattering potential as the sum of Coulomb and proximity potential, with considerations to shape degrees of freedom. The computed fusion cross sections for the reactions of ^{16}O on ^{144,147,148,149,150,152,154}Sm are compared with experimental data and coupled channel calculations using the code CCFULL. At and above the barrier the computed fusion cross sections match well with the experimental data, whereas below the barrier, calculations with nuclear surface tension coefficient improved by Reisdorf in the proximity potential with considerations to shape degrees of freedom give reasonably good fit. The good agreement between theory and experiment in the case of ^{16}O on ^{144,147,148,149,150,152,154}Sm reactions is equally valid in the prediction of the fusion of ^{16}O on ^{145,146,151,153}Sm. Reduced reaction cross sections for the fusion of ^{16}O on ^{145,146,152,154}Sm have also been described.

Keywords: heavy-ion reactions, sub-barrier fusion, barrier penetration model.

PACS: 25.70.Jj, 24.10.Eq, 21.60.Ev, 27.60. +j, 27.70.+q

1. INTRODUCTION

Wide and in-depth experimental and theoretical studies of heavy-ion fusion reactions in low energy range at, above and below the Coulomb barrier [1–10] have been an area of extensive investigations for many years in Nuclear Physics. The observations in heavy-ion systems at the near and the Coulomb barrier energies are quite important for the understanding of the complexity of collision processes at low energies, especially in the search of super heavy elements (SHE) [11, 12]. In the analysis of heavy-ion fusion reactions, the inter-nuclear interaction, consisting of repulsive Coulomb and centrifugal potentials and attractive nuclear potential which are functions of the distance between center-of mass of the colliding nuclei plays a major role. The total potential attains a maximum value at a distance

beyond the touching configuration where the repulsive Coulomb force and the attractive nuclear forces balance each other and when the energy of relative motion overcomes this potential barrier, the nuclei gets captured and fused.

Even though the simple one dimension barrier penetration model [1] explains the fusion reactions of heavy-ions above the barrier, the large enhancement in the fusion cross-sections below the barrier in several orders of magnitude over those expected from the simple one dimension barrier penetration model can only be explained in terms of coupling of relative motion to internal degrees of freedom of the colliding nuclei such as deformation [4, 13, 14], vibration [15–18], and nucleon transfer channels [19–22] or related to the gross features of nuclear matter such as neck formation [23, 24] between the two colliding nuclei.

In our previous work [10], the fusion excitation functions for the fusion of ^{12}C, ^{16}O, ^{28}Si and ^{35}Cl on ^{92}Zr have been calculated using one-dimensional barrier penetration model, taking the scattering potential as the sum of Coulomb and proximity potential and are compared with experimental data and coupled channel calculations using code CCFULL, without considering shape degrees of freedom. In the present work, the fusion excitation functions for the fusion of ^{16}O on $^{144\text{-}154}$Sm have been calculated using one-dimensional barrier penetration model, taking scattering potential as the sum of Coulomb and proximity potential [25] and the calculated values of ^{16}O on ^{144,147,148,149,150,152,154}Sm are compared with experimental data [26] and coupled channel calculations using the code CCFULL [6], with considerations to shape degrees of freedom. In the Coulomb and proximity potentials, the quadrupole and the hexadecapole deformation values of the projectile and target nuclei, the angular momentum effects and hence the vibrational couplings have been considered. In the CCFULL calculations we have given considerations to vibrational couplings in the projectile and the target, with deformation parameters $\beta_\lambda^N = \beta_\lambda^C$. Reduced reaction cross sections for the fusion of ^{16}O on ^{145,146,150,152}Sm have also been described, by using the usual reduction procedure of dividing the cross section by πR_0^2, where R_0 is the barrier radius and the division of energy by Coulomb barrier.

In the case of reactions of ^{16}O on $^{144\text{ -}154}$Sm, it is to be noted that the target Sm nuclei are known to exhibit a wide range of deformation from most stable spherical semi magic ^{144}Sm to the well deformed ^{154}Sm, where as the projectile ^{16}O is doubly magic.

2. THEORY

2.1. THE POTENTIAL

Discovering a unique nuclear potential that can be used exclusively for probing different reaction mechanisms on a single platform is obviously a tough

nut for the last several years in nuclear physics. In order to incorporate the role of different colliding nuclei in the nuclear potential, it is commonly accepted that the potential can be written as a product of geometrical factor (proportional to the reduced radii of colliding nuclei) and a universal function. In this effort, the proximity potential of Blocki *et al.* [27], which is free of adjustable parameters and makes use of the measured values of the nuclear surface tension and surface diffuseness, provides a simple formula for the nucleus-nucleus interaction energy as a function of separation between the surfaces of the approaching nucleus.

The interaction barrier for two colliding nuclei is given as:

$$V = \frac{Z_1 Z_2 e^2}{r} + V_P(z) + \frac{\hbar^2 \ell(\ell+1)}{2\mu r^2}, \tag{1}$$

where Z_1 and Z_2 are the atomic numbers of projectile and target, r is the distance between the centers of the projectile and target, z is the distance between the near surfaces of the projectile and target, ℓ is the angular momentum, μ is the reduced mass of the target and projectile and $V_P(z)$ is the proximity potential given as:

$$V_P(z) = 4\pi\gamma b \frac{C_1 C_2}{C_1 + C_2} \phi(\frac{z}{b}), \tag{2}$$

with the nuclear surface tension coefficient

$$\gamma = 0.9517[1 - 1.7826(N-Z)^2 / A^2], \tag{3}$$

ϕ, the universal proximity potential is given as:

$$\phi(\xi) = -4.41\exp(-\xi/0.7176), \quad \text{for } \xi \geq 1.9475 \tag{4}$$

$$\phi(\xi) = -1.7817 + 0.9270\xi + 0.01696\xi^2 - 0.05148\xi^3, \quad \text{for } 0 \leq \xi \leq 1.9475 \tag{5}$$

$$\phi(\xi) = -1.7817 + 0.9270\xi + 0.0143\xi^2 - 0.09\xi^3, \quad \text{for } \xi \leq 0, \tag{6}$$

with $\xi = z/b$, where the width (diffuseness) of nuclear surface $b \approx 1$ and Siissmann Central radii C_i related to sharp radii R_i as $C_i = R_i - \frac{b^2}{R_i}$. For R_i, we use the semi empirical formula in terms of mass number A_i as:

$$R_i = 1.28A_i^{1/3} - 0.76 + 0.8A_i^{-1/3}. \tag{7}$$

During the last three decades several attempts have been made to improve the proximity potential [28, 29]. In these works an improved version of nuclear surface tension co-efficient is presented by Reisdorf as:

$$\gamma = 1.2496[1 - 2.3(N - Z)^2 / A^2]. \quad (8)$$

The choice of the potential and its form to be adopted is one of the most challenging aspects, when one wants to compare the experimental fusion data with theory, both below and above the barrier.

2.2. THE FUSION CROSS SECTION

To describe the fusion reactions at energies not too much above the barrier and at higher energies, the barrier penetration model developed by C. Y. Wong [1] has been widely used for the last four decades, which obviously explains the experimental result properly. Following Thomas [30], Huizenga and Igo [31] and Rasmussen and Sugawara [32], Wong approximated the various barriers for different partial waves by inverted harmonic oscillator potentials of height E_ℓ and frequency ω_ℓ. For energy E, using the probability for the absorption of ℓ^{th} partial wave given by Hill-Wheeler formula [33], Wong arrived at the total cross section for the fusion of two nuclei by quantum mechanical penetration of simple one-dimensional potential barrier as:

$$\sigma = \frac{\pi}{k^2} \sum_\ell \frac{2\ell + 1}{1 + \exp[2\pi(E_\ell - E)/\hbar\omega_\ell]}, \quad (9)$$

where $k = \sqrt{\frac{2\mu E}{\hbar^2}}$. Here $\hbar\omega_\ell$ is the curvature of the inverted parabola. Using some parameterizations in the region $\ell = 0$ and replacing the sum in Eq. (9) by an integral Wong gave the reaction cross section as:

$$\sigma = \frac{R_0^2 \hbar\omega_0}{2E} \ln\left\{1 + \exp\left[\frac{2\pi(E - E_0)}{\hbar\omega_0}\right]\right\}. \quad (10)$$

For relatively large values of E, the above result reduces to the well-known formula:

$$\sigma = \pi R_0^2 \left[1 - \frac{E_0}{E}\right]. \quad (11)$$

For relatively small values of E, such that $E << E_0$:

$$\sigma = \frac{R_0^2 \hbar\omega_0}{2E} \exp\left[2\pi(E - E_0)/\hbar\omega_0\right]. \quad (12)$$

Below the barrier, the tunneling through the barrier has to occur in order to allow the fusion of the two nuclei and in terms of partial wave; the fusion cross section is given as:

$$\sigma = \frac{\pi}{k^2} \sum_{\ell=0}^{\ell=\ell_C} (2\ell + 1)P, \tag{13}$$

where $\ell_C = R_a \sqrt{2\mu(E_{c.m} - V_{(R_a, \eta_{in}, \ell=0)})} \big/ \hbar$, R_a is the first turning point and η_{in} is the entrance channel asymmetry. Here, P is the WKB penetration probability given as:

$$P = \exp\left\{ -\frac{2}{\hbar} \int_a^b \sqrt{2\mu(V - E)} \mathrm{d}z \right\}, \tag{14}$$

where a and b are the inner and outer turning points defined as $V(a) = V(b) = E$.

In the case of deformed nuclei the penetration probability is different in different directions. The averaging of penetrability over different directions is done using the expression

$$P = \frac{1}{2} \int_0^{\pi} P(E, \theta, \ell) \sin(\theta) \mathrm{d}\theta, \tag{15}$$

where $P(E, \theta, \ell)$ is the penetrability in the direction of θ from the symmetry axis of the axially symmetric deformed nuclei.

The Coulomb interaction between the two deformed and oriented nuclei [1] with higher multipole deformation included [34–36] is given as,

$$V_C = \frac{Z_1 Z_2 e^2}{r} + 3Z_1 Z_2 e^2 \sum_{\lambda, i=1,2} \frac{1}{2\lambda + 1} \frac{R_i^{\lambda}}{r^{\lambda+1}} Y_{\lambda}^{(0)}(\alpha_i) \left[\beta_{\lambda i} + \frac{4}{7} \beta_{\lambda i}^2 Y_{\lambda}^{(0)}(\alpha_i) \delta_{\lambda,2} \right] \tag{16}$$

with

$$R_i(\alpha_i) = R_{0i} \left[1 + \sum_{\lambda} \beta_{\lambda i} Y_{\lambda}^0(\alpha_i) \right], \tag{17}$$

where $R_{0i} = 1.28 A_i^{1/3} - 0.76 + 0.8 A_i^{-1/3}$. Here α_i is the angle between the radius vector and symmetry axis of the i^{th} nuclei.

Fusion reactions at energies near and below the Coulomb barrier are strongly influenced by couplings of the relative motion of the colliding nuclei to several nuclear intrinsic motions; quantum tunneling in the presence of couplings has to be

considered. The FORTRAN77 program CCFULL solves the coupled channel equations in computing the fusion cross sections, taking into account the coupling between the relative motion and the intrinsic degrees of freedom.

2.3. THE REDUCED REACTION CROSS SECTION

In order to compare the excitation functions of different reaction mechanisms induced by different projectiles on the same target nucleus, the procedure of eliminating the geometrical factors concerning different systems by 'reducing' the cross section and the centre-of-mass energy has extensively been used in recent years [26, 37, 38]. The normal procedure consists of the division of the cross section by πR_0^2, where R_0 is the barrier radius and the division of energy by Coulomb barrier E_0.

3. RESULTS AND DISCUSSIONS

Interaction barrier for the fusion of ^{16}O on ^{144}Sm has been plotted in Fig.1, against the distance between the centers of the projectile and target while taking the scattering potential as the sum of Coulomb and proximity potentials. The dotted lines in Fig.1 represent the interaction barrier calculated using nuclear surface tension coefficient given by Eq.(3), denoted as γ-old and the dashed line represents the result while using Eq.(8), denoted as γ-new without considering the shape degrees of freedom of the projectile and target. The dash-dotted line and the solid line represent the barrier calculations using nuclear surface tension co-efficient given by Eq.(3) and Eq.(8) respectively with considerations to deformations, using Eq.(16) for $\ell = 0$. It should be noted that the barrier height E_0 increases and the barrier radius R_0 shifts towards smaller value, while considering the shape degrees of freedom for both normal and improved values surface tension coefficients given by Eq.(3) and Eq.(8) respectively. In the both cases of with and without deformations the barrier height E_0 decreases and the barrier radius R_0 shifts towards larger value with improved value of surface tension coefficient given by Eq. (8) than the normal value given by Eq.(3). Moreover, Eq. (8) gives deeper potential compared to Eq. (3).

At, above and below the barrier, the total fusion cross-sections for the reactions of ^{16}O on $^{144\text{-}154}$Sm have been calculated by using the values of barrier height E_0 and barrier radius R_0 taken from the respective figures corresponding to Fig.1 and using Eqs. (9) to (16). The calculated fusion cross sections for the reactions of ^{16}O on ^{144,147,148,149,150,152,154}Sm are compared with experimental data [24] and CCFULL calculations. In all CCFULL calculations the dotted lines represent calculations

using no channel couplings and the solid lines represent the vibrational couplings in projectile and target, while using the code CCFULL with deformation parameters, $\beta_\lambda^N = \beta_\lambda^C$. The depth parameter V_0 and the surface diffuseness parameter a_0 (of the Wood-Saxon potentials) have been computed [39], with r_0 fixed at 1.20 fm and the values are shown in Table 1. While using the vibrational couplings in projectile, the single phonon excitation in ^{16}O with $\beta_3^N = 0.353$ and excitation energy $\varepsilon_3 = 6.13$ MeV of 3^- state is used, whereas pair transfer channel is not included.

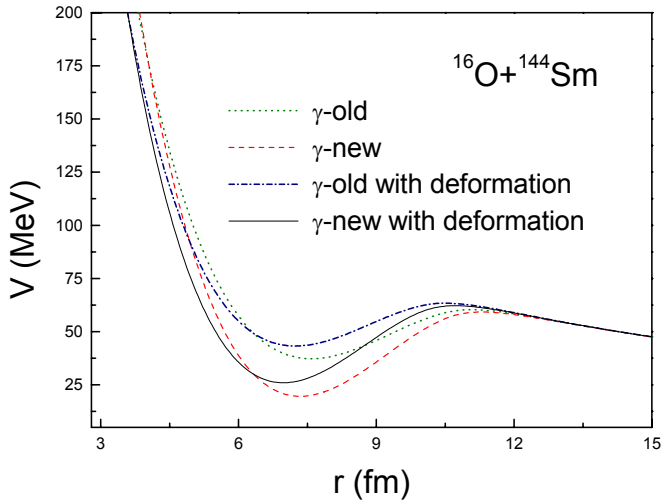

Fig.1 – Scattering potential (color online) for the projectile ^{16}O on ^{144}Sm target consisting of repulsive Coulomb and centrifugal potentials and attractive nuclear potential.

In Fig. 2a, in the case of reaction of doubly magic ^{16}O on most stable spherical semi magic ^{144}Sm target, the fusion cross sections (up triangles) computed using Wong's formula given by Eq. (9) with Coulomb and proximity potential and nuclear surface tension coefficient given by Eq. (3), denoted as γ-old, fit very well with the experimental data (circles) above the barrier, whereas below the barrier show some disagreement. Above the barrier, it is to be noted that no appreciable change in the fusion cross sections (open diamonds) have been observed while recalculating the fusion cross sections, with considerations to shape degrees of freedom as per Eq.(16) and using Eq.(11). Below the barrier, we have considered the fusion process as a tunneling process and the cross sections (open diamonds) calculated using Eqs. (3), (13) and (16) show good agreement with the experimental data (circles), while using Coulomb and proximity potential. Here in the CCFULL calculations (Coupled) the single phonon excitation with $\beta_3^N = 0.0881$ and excitation energy 1.81MeV of 3^- state in ^{144}Sm is used.

Using a similar procedure, we have calculated the fusion cross sections for the reactions of ^{16}O projectile on ^{145}Sm target and the corresponding excitation functions are shown in Fig. 2b. In Fig. 2b, the up triangles represent the fusion cross sections calculated using Wong's formula given by Eq.(9) and the open diamonds represent the calculations using Eqs.(11), (13) and (16). In both cases nuclear surface coefficient given by Eq.(3) has been used, in the proximity potential. Fig. 2c represents the excitation functions for the reactions of ^{16}O projectile on ^{146}Sm target with surface tension coefficient given by Eq. (3).

In the case of reaction of ^{16}O projectile on ^{147}Sm target, which is the closest stable isotope to semi magic ^{144}Sm, for getting a better result, we have changed the nuclear surface tension co-efficient given by Eq. (3) in the proximity potential by Eq. (8), denoted as γ-new and recalculated all the cross sections, following a similar procedure. The computed results with Eq.(8) show better agreement with the experimental data than the results while using the surface tension coefficient given by Eq. (3). While using γ-new, the computed cross sections with Wong's formula given by Eq.(9) (up triangles), cross sections computed with Eqs.(11), (13) and (16) (open diamonds), the CCFULL calculations (solid line and dotted line) and the experimental cross sections (circles) are shown in Fig.2d. In the coupled channel calculations the single phonon excitation with $\beta_2^N = 0.143$ and excitation energy of 0.121MeV of ^{147}Sm has been used. In Fig. 2d, the computed cross sections with Eqs.(11), (13) and (16) (open diamonds) show good agreement with experimental data (circles).

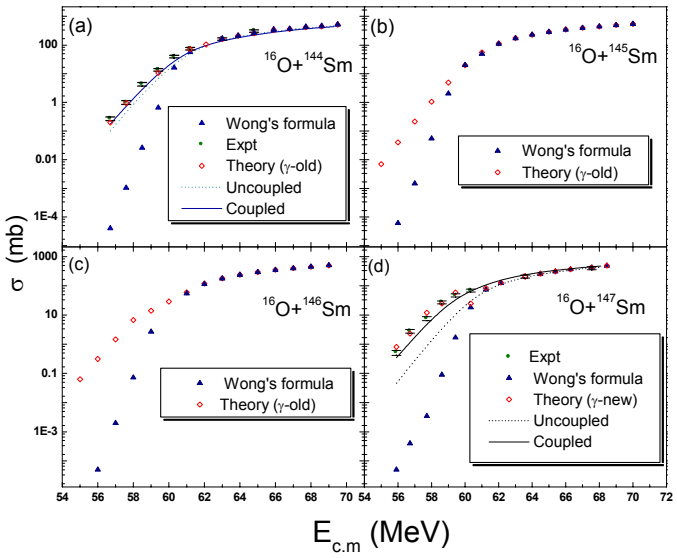

Fig. 2 – Fusion excitation functions (color online) for the reactions of ^{16}O projectile on $^{144-147}$Sm targets. In Figs. 2a and 2d, the comparison of the computed fusion cross sections with experiment and CCFULL calculations are shown.

Figs. 3a, 3b, 3c, 4a and Fig. 5 show the comparison of experimental fusion cross sections with calculations while using Wong's formula given by Eq.(9), calculations with Eqs.(10), (13) to (16) and the CCFULL calculations, in the case of reactions of ^{16}O on ^{148,149,150,152}Sm and well deformed ^{154}Sm targets. In all the cases the nuclear surface tension coefficients given by Eq.(8) has been used, in the proximity potential. In the CCFULL calculations (Coupled), for single phonon couplings in ^{148}Sm,^{150}Sm, ^{152}Sm and ^{154}Sm, the β_3^N values and the corresponding excitation energies of 3^- state are shown in Table 2. In the case of ^{149}Sm target the single phonon excitation with $\beta_2^N = 0.180$ and excitation energy of 0.022MeV has been used.

Table 1

Depth parameter V_0 and the surface diffuseness parameter a_0 for the reaction of ^{16}O on various Sm targets

Reaction	V_0 (MeV)	a_0 (fm)
^{16}O+^{144}Sm	61.98	0.6517
^{16}O+^{147}Sm	62.15	0.6520
^{16}O+^{148}Sm	62.20	0.6521
^{16}O+^{149}Sm	62.26	0.6522
^{16}O+^{150}Sm	62.32	0.6524
^{16}O+^{152}Sm	62.42	0.6526
^{16}O+^{154}Sm	62.53	0.6528

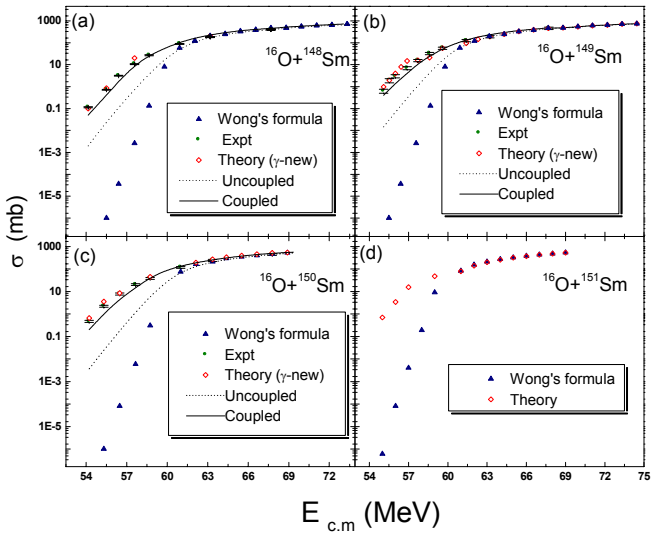

Fig. 3 – Fusion excitation functions (color online) for the reactions of ^{16}O projectile on $^{148-151}$Sm targets, where a), b), c) show the comparison of the computed fusion cross sections with experiment and CCFULL calculations are shown.

Table 2

β_3^N values and the corresponding excitation energies of 3^- states of ^{148}Sm, ^{150}Sm, ^{152}Sm and ^{154}Sm targets

Target	β_3^N value	Excitation energy (MeV)
^{148}Sm	0.142	1.161
^{150}Sm	0.193	1.071
^{152}Sm	0.307	1.041
^{154}Sm	0.339	1.012

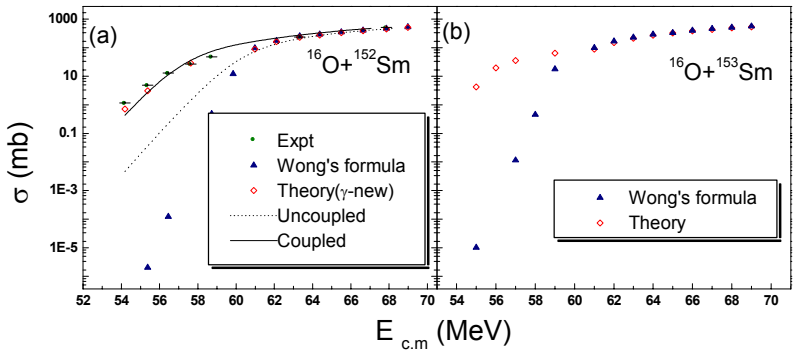

Fig. 4 – Fusion excitation functions (color online) for the reactions of ^{16}O projectile on ^{152}Sm and ^{153}Sm targets. In Fig. 4a, the comparison of the computed fusion cross sections with experiment and CCFULL calculations is shown.

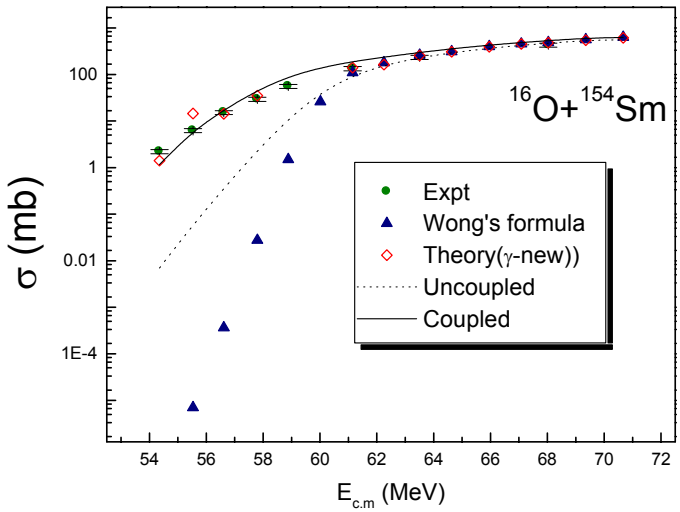

Fig. 5 – The comparison (color online) of the computed fusion cross sections of ^{16}O + ^{154}Sm with experiment and CCFULL calculations.

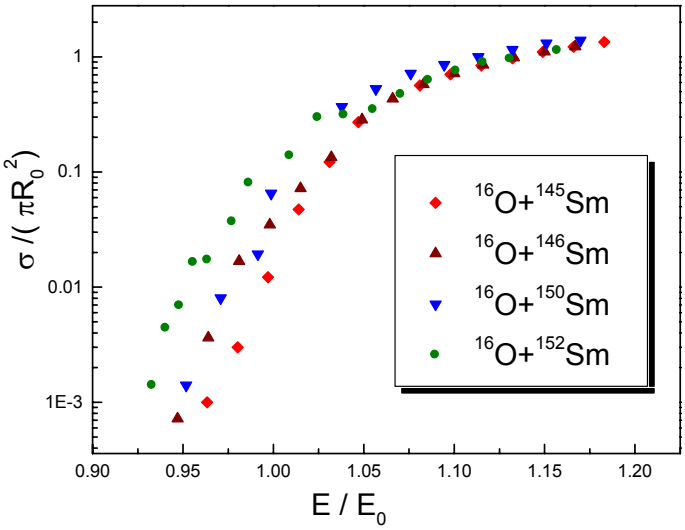

Fig. 6 – Reduced reaction (color online) cross sections for ^{16}O + ^{145,146,150,152}Sm systems.

The good agreement between theory and experiment in the case of ^{16}O on ^{144,147,148,149,150,152,154}Sm reactions be equally valid in the case of ^{16}O on ^{145,146,151,153}Sm reactions as shown in Figs. 2b,c, 3d and 4b, that predict those fusion reactions easily.

Fig. 6 represents reduced reaction cross sections for the systems ^{16}O + ^{145,146,150,152}Sm by the reduction procedure of dividing the cross section by πR_0^2 and the energy by E_0. It should be noted that the reduced reaction cross sections compare the fusion reactions easily in the same figure. Well above the barrier the reactions cross section almost matches for all the reactions, whereas below the barrier the reaction cross section is largest for ^{16}O + ^{152}Sm system followed by ^{16}O + ^{150,146,145}Sm systems.

4. CONCLUSIONS

At and above the barrier, the simple one dimension barrier penetration model developed by Wong explains the fusion reactions of heavy ions very well, while using the scattering potential as the sum of Coulomb and proximity potentials, irrespective of even-even or even-odd nuclei. The enhancements in fusion cross sections below the Coulomb barrier orders of magnitude larger than the predictions of one dimension barrier penetration model reveals the important role played by nuclear structure of the colliding nuclei. Below the barrier larger deformations corresponds to large sub barrier enhancement of fusion cross sections.

Below the barrier the fusion process can be considered as a tunneling process and in the quantum mechanical tunneling of one dimension barrier penetration model the inclusion of nuclear deformation parameters in Coulomb and proximity potential model explains the nuclear fusion cross sections of both even-even and even-odd nuclei very well, irrespective of other structural effects like zero point oscillations of nuclear shape, the presence of unpaired neutron in the nuclei etc. In the calculation of interaction barrier of deformed nuclei, the nuclear surface tension coefficient given by Reisdorf shows better results than the usual surface tension coefficient of proximity potential. The reduced cross sections compare different fusion reaction mechanisms induced by different targets with the same projectiles in the same figure.

REFERENCES

1. C. Y. Wong, Phys. Rev. Lett., **31**, 766 (1973).
2. N. Rowley, G. R. Satchler and P. H. Stelson, Phys. Lett. B, **254**, 25 (1991).
3. R. K. Puri and R. K. Gupta, Phys. Rev. C, **45**, 1837 (1992).
4. J. R. Leigh, M. Dasgupta, D. J. Hinde, J. C. Mein, C. R. Morton, R. C. Lemmon, J. P. Lestone, J. O. Newton, H. Timmers, J. X. Wei and N. Rowley, Phys. Rev. C, **52**, 3151 (1995).
5. H. Timmers, J. R. Leigh, N. Rowley, A. M. Stefanini, D. Ackermann, S. Beghini, L. Corradi, M. Dasgupta, J. H. He, D. J. Hinde, J. C. Mein, G. Montagnoli, C. R. Morton, J. O. Newton, F. Scarlassara and G. F. Segato, J.Phys.G: Nucl.Part.Phys., **23**, 1175 (1997).
6. K. Hagino, N. Rowley and A. T. Kruppa, Comput.Phys.Commun., **123**, 143 (1999).
7. J. O. Newton, R. D. Butt, M. Dasgupta, D. J. Hinde, I. I. Gontchar and C. R. Morton, Phys. Rev. C, **70**, 024605 (2004).
8. P. R. S. Gomes, I. Padron, E. Crema, O. A. Capurro, F. Niello, A. Arazi, G. V. Marti, J. Lubian, M. Trotta, A. J. Pacheco, J. E. Testoni, M. D. Rodriguez, M. E. Ortega, L. C. Chamon, R. M. Anjos, R. Veiga, M. Dasgupta, D. J. Hinde and K. Hagino, Phys. Rev. C, **73**, 064606 (2006).
9. N. Wang, Z. Li and W. Scheid, J.Phys.G:Part.Phys., **34**, 1935 (2007).
10. K. P. Santhosh, V. Bobby Jose, Antony Joseph and K. M. Varier, Nucl. Phys. A, **817**, 35 (2009).
11. G.G. Adamian, N.V. Antonenko, W. Scheid, Rom. J. Phys., **57**, 9 (2012).
12. S. Hofman, Rom. J. Phys., **57**, 214 (2012).
13. J. D. Bierman, P. Chan, J. F. Liang, M. P. Kelly, A. A. Sonzogni and R. Vandenbosch, Phys. Rev. Lett., **76**, 1587 (1996).
14. R. G. Stokstadand and E. E. Gross, Phys. Rev. C, **23**, 281 (1981).
15. A. M. Stefanini, G. Fortuna, A. Tivelli, W. Meczynski, S. Beghini, C. Signorini, S. Lunardi and M. Morando, Phys. Rev. C, **30**, 2088 (1984).
16. A.M. Stefanini, D. Ackermann, L. Corradi, J. H. He, G. Montagnoli, S. Beghini, F. Scarlassara and G. F. Segato, Phys. Rev. C, **52**, R1727 (1995).
17. J. O. Newton, C. R. Morton, M. Dasgupta, J. R. Leigh, J. C. Mein, D. J. Hinde, H. Timmers and K. Hagino, Phys. Rev. C, **64**, 064608 (2001).
18. A. M. Stefanini, D. Ackermann, L. Corradi, D. R Napoli, C. Petrache, P. Spolaore, P. Bednarczyk and H. Q. Zhang, Phys. Rev. Lett., **74**, 864 (1995).
19. V. I. Zagrebaev, Phys. Rev. C, **67**, 061601 (2003).
20. V. Yu. Denisov, Eur. Phys. J. A, **7**, 87 (2000).
21. V. Tripathi, L. T. Baby, J. J. Das, P. Sugathan, N. Madhavan, A. K. Sinha, P. V. Madhusudhana Rao, S. K. Hui, R. Sing and K. Hagino, Phys. Rev. C, **65** (2001).

22. L. T. Baby, V. Tripathi, D. O. Kataria, J. J. Das, P. Sugathan, N. Madhavan, A. K. Sinha, M. C. Radhakrishna, N. M. Badiger, N. G. Puttaswamy, A. M. Vinodkumar and N. V. S. V. Prasad, Phys. Rev. C, **56**, 1936 (1997).
23. C. E. Aguiar, V. C. Barbosa, L. F. Canto and R. Donangelo, Nucl. Phys. A, **472**, 571 (1987).
24. C. E. Aguiar, L. F. Canto and R. Donangelo, Phys. Rev. C, **31**, 1969 (1985).
25. K.P. Santhosh and V. Bobby Jose, Nucl. Phys. A, **922**, 191 (2014).
26. D. E. DiGregorio, M. diTada, D. Abriola, M. Elgue, A. Etchegoyen, M. C. Etchegoyen, J. O. Fernandez Niello, A.M.Ferrero, S. Gil, A. O. Macchiavelli, A. J. Pacheco, J. E. Testoni, P. R. Silveira Gomes, V. R. Vanin, R. Liguori Neto, E. Crema and R. G. Stokstad, Phys. Rev. C, **39**, 516 (1989).
27. J. Blocki, J. Randrup, W. J. Swiatecki and C. F. Tsang, Ann. Phys. (N.Y), **105**, 427 (1977).
28. W. Reisdorf, J. Phys. G: Nucl. Part. Phys., **20**, 1297 (1994).
29. W. D. Myers and W. J. Swiatecki, Phys. Rev. C, **62**, 044610 (2000).
30. T. D. Thomas, Phys. Rev., **116**, 703 (1959).
31. J. Huizenga and G. Igo, Nucl. Phys., **29**, 462 (1961).
32. J. Rasmussen and K. Sugawara-Tanabe, Nucl. Phys.,A **171**, 497 (1971).
33. D. L. Hill and J. A. Wheeler, Phys. Rev., **89**, 1102 (1953) 1102.
34. N. Malhotra and R. K. Gupta, Phys Rev., C **31**, 1179 (1985).
35. R. K. Gupta, M. Balasubramaniam, R. Kumar, N. Singh, M. Manhas and W Greiner, J. Phys. G: Nucl. Part. Phys., **31**, 631 (2005).
36. M. Bansal, R. K. Gupta, Rom. J. Phys., **57**, 18 (2012).
37. M. Beckerman, M. Salomaa, A. Sperduto, J. D. Molitoris and A. DiRienzo, Phys. Rev. C, **25**, 837 (1982).
38. D. E. DiGregorio, J. O. Fernandez Niello, A. J. Pacheco, D. Abriola, S. Gil, A. O. Macchiavelli, J. E. Testoni, P.R.Pascholati, V. R. Vanin, R. Liguori Neto, N. Carlin Filho, M. M. Coimbra, P. R. S. Gomes and R. G. Stokstad, Phys. Lett. B, **176**, 322 (1986).
39. A Winther, Nucl. Phys. A, **594**, 203 (1995).